We are IntechOpen, the world's leading publisher of Open Access books Built by scientists, for scientists

4,800
Open access books available

122,000
International authors and editors

135M
Downloads

Our authors are among the

154
Countries delivered to

TOP 1%
most cited scientists

12.2%
Contributors from top 500 universities

CLARIVATE ANALYTICS BOOK CITATION INDEX INDEXED

WEB OF SCIENCE™

Selection of our books indexed in the Book Citation Index in Web of Science™ Core Collection (BKCI)

Interested in publishing with us?
Contact book.department@intechopen.com

Numbers displayed above are based on latest data collected.
For more information visit www.intechopen.com

5

Passive permanent magnet bearings for rotating shaft : Analytical calculation

Valerie Lemarquand*
LAPLACE. UMR5213. Universite de Toulouse
France

Guy Lemarquand†
LAUM. UMR6613. Universite du Maine
France

1. Introduction

Magnetic bearings are contactless suspension devices, which are mainly used for rotating applications but also exist for translational ones. Their major interest lies of course in the fact that there is no contact and therefore no friction at all between the rotating part and its support. As a consequence, these bearings allow very high rotational speeds. Such devices have been investigated for eighty years. Let's remind the works of F. Holmes and J. Beams (Holmes & Beams, 1937) for centrifuges.
The appearing of modern rare earth permanent magnets allowed the developments of passive devices, in which magnets work in repulsion (Meeks, 1974)(Yonnet, 1978).
Furthermore, as passive magnetic bearings don't require any lubricant they can be used in vacuum and in very clean environments.
Their main applications are high speed systems such as turbo-molecular pumps, turbo-compressors, energy storage flywheels, high-speed machine tool spindles, ultra-centrifuges and they are used in watt-hour meters and other systems in which a very low friction is required too (Hussien et al., 2005)(Filatov & Maslen, 2001).

The magnetic levitation of a rotor requires the control of five degrees of freedom. The sixth degree of freedom corresponds to the principal rotation about the motor axis. As a consequence of the Earnshaw's theorem, at least one of the axes has to be controlled actively. For example, in the case of a discoidal wheel, three axes can be controlled by passive bearings and two axes have to be controlled actively (Lemarquand & Yonnet, 1998). Moreover, in some cases the motor itself can be designed to fulfil the function of an active bearing (Barthod & Lemarquand, 1995). Passive magnetic bearings are simple contactless suspension devices but it must be emphazised that one bearing controls a single degree of freedom. Moreover, it exerts only a stiffness on this degree of freedom and no damping.

*valerie.lemarquand@ieee.org
†guy.lemarquand@ieee.org

Permanent magnet bearings for rotating shafts are constituted of ring permanent magnets. The simplest structure consists either of two concentric rings separated by a cylindrical air gap or of two rings of same dimensions separated by a plane air gap. Depending on the magnet magnetization directions, the devices work as axial or radial bearings and thus control the position along an axis or the centering of an axis. The several possible configurations are discussed throughout this chapter. The point is that in each case the basic part is a ring magnet. Therefore, the values of importance are the magnetic field created by such a ring magnet, the force exerted between two ring magnets and the stiffness associated.

The first author who carried out analytical calculations of the magnetic field created by ring permanent magnets is Durand (Durand, 1968). More recently, many authors proposed simplified and robust formulations of the three components of the magnetic field created by ring permanent magnets (Ravaud et al., 2008)(Ravaud, Lemarquand, Lemarquand & Depollier, 2009)(Babic & Akyel, 2008a)(Babic & Akyel, 2008b)(Azzerboni & Cardelli, 1993).
Moreover, the evaluation of the magnetic field created by ring magnets is only a helpful step in the process of the force calculation. Indeed, the force and the stiffness are the values of importance for the design and optimization of a bearing. So, authors have tried to work out analytical expressions of the force exerted between two ring permanent magnets (Kim et al., 1997)(Lang, 2002)(Samanta & Hirani, 2008)(Janssen et al., 2010)(Azukizawa et al., 2008).
This chapter intends to give a detailed description of the modelling and approach used to calculate analytically the force and the stiffness between two ring permanent magnets with axial or radial polarizations (Ravaud, Lemarquand & Lemarquand, 2009a)(Ravaud, Lemarquand & Lemarquand, 2009b). Then, these formulations will be used to study magnetic bearings structures and their properties.

2. Analytical determination of the force transmitted between two axially polarized ring permanent magnets.

2.1 Preliminary remark

The first structure considered is shown on Fig.1. It is constituted of two concentric axially magnetized ring permanent magnets. When the polarization directions of the rings are antiparallel, as on the figure, the bearing controls the axial position of the rotor and works as a so called axial bearing. When the polarization directions are the same, then the device controls the centering around the axis and works as a so called radial bearing. Only one of the two configurations will be studied thoroughly in this chapter because the results of the second one are easily deducted from the first one. Indeed, the difference between the configurations consists in the change of one of the polarization direction into its opposite. The consequence is a simple change of sign in all the results for the axial force and for the axial stiffness which are the values that will be calculated.
Furthermore, the stiffness in the controlled direction is often considered to be the most interesting value in a bearing. So, for an axial bearing, the axial stiffness is the point. Nevertheless, both stiffnesses are linked. Indeed, when the rings are in their centered position, for symmetry reasons, the axial stiffeness, K_z, and the radial one, K_r, verify:

$$2K_r + K_z = 0 \tag{1}$$

So, either the axial or the radial force may be calculated and is sufficient to deduct both stiffnesses. Thus, the choice was made for this chapter to present only the axial force and stiffness in the sections dealing with axially polarized magnets.

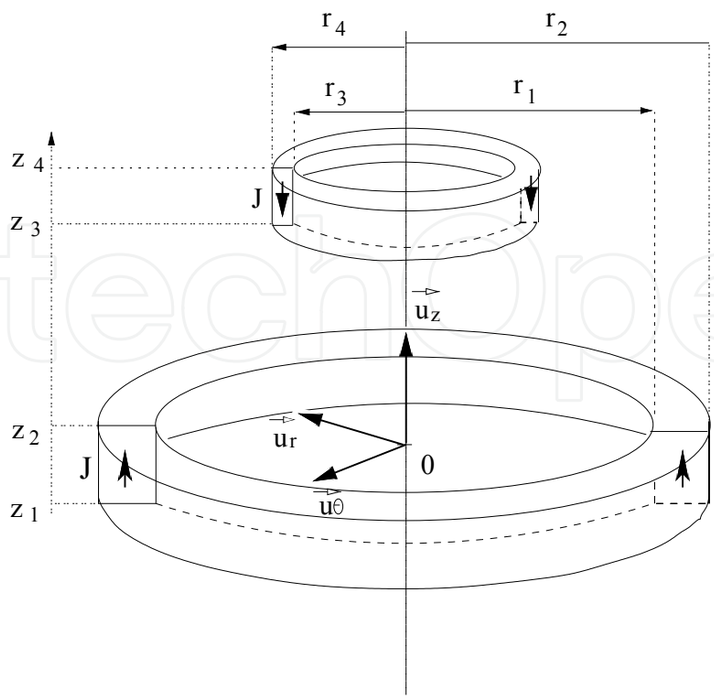

Fig. 1. Axial bearing constituted of two axially magnetized ring permanent magnets. J_1 and J_2 are the magnet polarizations

2.2 Notations

The parameters which describe the geometry of Fig.1 and its properties are listed below:
J_1: outer ring polarization [T].
J_2: inner ring polarization [T].
r_1, r_2: radial coordinates of the outer ring [m].
r_3, r_4: radial coordinates of the inner ring [m].
z_1, z_2: axial coordinates of the outer ring [m].
z_3, z_4: axial coordinates of the inner ring [m].
$h_1 = z_2 - z_1$: outer ring height [m].
$h_2 = z_4 - z_3$: inner ring height [m].
The rings are radially centered and their polarizations are supposed to be uniform.

2.3 Magnet modelling

The axially polarized ring magnet has to be modelled and two approaches are available to do so. Indeed, the magnet can have a coulombian representation, with fictitious magnetic charges or an amperian one, with current densities. In the latter, the magnet is modelled by two cylindrical surface current densities k_1 and k_2 located on the inner and outer lateral surfaces of the ring whereas in the former the magnet is modelled by two surface charge densities located on the plane top and bottom faces of the ring.
As a remark, the choice of the model doesn't depend on the nature of the real magnetic source, but is done to obtain an analytical formulation. Indeed, the authors have demontrated

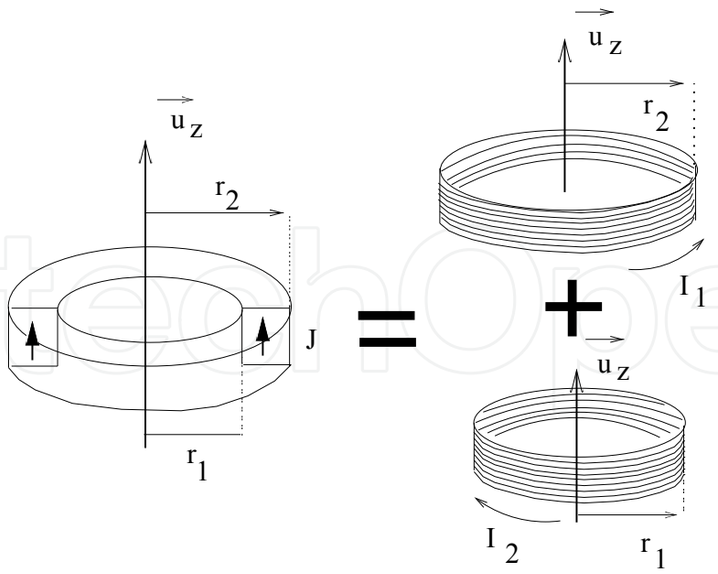

Fig. 2. Model of a ring magnet: amperian equivalence.

that depending on the polarization direction of the source only one of the model generally yields an analytical formulation. So, the choice rather depends on the considered problem.

2.4 Force calculation

The force transmitted between two axially polarized ring permanent magnets is determined by using the amperian approach. Thus, each ring is replaced by two coils of N_1 and N_2 turns in which two currents, I_1 and I_2, flow. Indeed, a ring magnet whose polarization is axial and points up, with an inner radius r_1 and an outer one r_2, can be modelled by a coil of radius r_2 with a current I_2 flowing anticlockwise and a coil of radius r_1 with a current I_1 flowing clockwise (Fig.2).
The equivalent surface current densities related to the coil heights h_1 and h_2 are defined as follows for the calculations:
$k_1 = N_1 I_1 / h_1$: equivalent surface current density for the coils of radii r_1 and r_2.
$k_2 = N_2 I_2 / h_2$: equivalent surface current density for the coils of radii r_3 and r_4.

The axial force, F_z, created between the two ring magnets is given by:

$$F_z = \frac{\mu_0 k_1 k_2}{2} \sum_{i=1}^{2} \sum_{j=3}^{4} (-1)^{1+i+j} \left\{ f_z(r_i, r_j) \right\} \tag{2}$$

with

$$f_z(r_i, r_j) = r_i r_j \int_{z_3}^{z_4} \int_{z_1}^{z_2} \int_{0}^{2\pi} \frac{(\tilde{\tilde{z}} - \tilde{z}) \cos(\tilde{\theta}) d\tilde{z} d\tilde{z} d\tilde{\theta}}{\left(r_i^2 + r_j^2 - 2 r_i r_j \cos(\tilde{\theta}) + (\tilde{\tilde{z}} - \tilde{z})^2 \right)^{\frac{3}{2}}}$$

Parameter	Definition
β	$\frac{b+c}{b-c}$
μ	$\frac{c}{b+c}$
ϵ	$\frac{c}{c-b}$

Table 1. Parameters in the analytical expression of the force exerted between two axially polarized ring magnets.

The current densities are linked to the magnet polarizations by:

$$k_1 = \frac{J_1}{\mu_0} \tag{3}$$

and

$$k_2 = \frac{J_2}{\mu_0} \tag{4}$$

Then the axial force becomes:

$$F_z = \frac{J_1 J_2}{2\mu_0} \sum_{i,k=1}^{2} \sum_{j,l=3}^{4} (-1)^{(1+i+j+k+l)} F_{i,j,k,l} \tag{5}$$

with

$$F_{i,j,k,l} = r_i r_j g\left(z_k - z_l, r_i^2 + r_j^2 + (z_k - z_l)^2, -2r_i r_j\right) \tag{6}$$

$g(a,b,c) = A + S$

$$A = \frac{a^2-b}{c}\pi + \frac{\sqrt{c^2-(a^2-b)^2}}{c}\left(\log\left[\frac{-16c^2}{(c^2-(a^2-b)^2)^{(\frac{3}{2})}}\right] + \log\left[\frac{c^2}{(c^2-(a^2-b)^2)^{(\frac{3}{2})}}\right]\right)$$

$$\begin{aligned} S &= \frac{2ia}{c\sqrt{b+c}}\left((b+c)\mathbf{E}\left[\arcsin\left[\sqrt{\beta},\beta^{-1}\right]\right] - c\mathbf{F}\left[\arcsin\left[\sqrt{\beta},\beta^{-1}\right]\right]\right) \\ &+ \frac{2a}{c\sqrt{b-c}\sqrt{\epsilon}}\left(\frac{c}{\sqrt{\mu}}\mathbf{E}\left[\beta^{-1}\right] - c\sqrt{\mu}\mathbf{K}\left[\beta^{-1}\right]\right) \\ &+ \sqrt{\epsilon\beta^{-1}}\left((b-a^2)\mathbf{K}\left[2\mu\right] + (a^2-b+c)\mathbf{\Pi}\left[\frac{2c}{b+c-a^2}, 2\mu\right]\right) \end{aligned} \tag{7}$$

The special functions used are defined as follows:
$\mathbf{K}[m]$ is the complete elliptic integral of the first kind.

$$\mathbf{K}[m] = \int_0^{\frac{\pi}{2}} \frac{1}{\sqrt{1-m\sin(\theta)^2}} d\theta \tag{8}$$

$\mathbf{F}[\phi, m]$ is the incomplete elliptic integral of the first kind.

$$\mathbf{F}[\phi, m] = \int_0^{\phi} \frac{1}{\sqrt{1 - m\sin(\theta)^2}} d\theta \tag{9}$$

$\mathbf{E}[\phi, m]$ is the incomplete elliptic integral of the second kind.

$$\mathbf{E}[\phi, m] = \int_0^{\phi} \sqrt{1 - m\sin(\theta)^2} d\theta \tag{10}$$

$$\mathbf{E}[m] = \int_0^{\frac{\pi}{2}} \sqrt{1 - m\sin(\theta)^2} d\theta \tag{11}$$

$\mathbf{\Pi}[n, m]$ is the incomplete elliptic integral of the third kind.

$$\mathbf{\Pi}[n, m] = \mathbf{\Pi}\left[n, \frac{\pi}{2}, m\right] \tag{12}$$

with

$$\mathbf{\Pi}[n, \phi, m] = \int_0^{\phi} \frac{1}{\sqrt{1 - n\sin(\theta)^2}} \frac{1}{\sqrt{1 - m\sin(\theta)^2}} d\theta \tag{13}$$

3. Exact analytical formulation of the axial stiffness between two axially polarized ring magnets.

The axial stiffness, K_z existing between two axially polarized ring magnets can be calculated by deriving the axial force transmitted between the two rings, F_z, with regard to the axial displacement, z:

$$K_z = -\frac{d}{dz} F_z \tag{14}$$

F_z is replaced by the integral formulation of Eq.5 and after some mathematical manipulations the axial stiffness can be written:

$$K_z = \frac{J_1 J_2}{2\mu_0} \sum_{i,k=1}^{2} \sum_{j,l=3}^{4} (-1)^{(1+i+j+k+l)} C_{i,j,k,l} \tag{15}$$

where

$$\begin{aligned} C_{i,j,k,l} &= 2\sqrt{\alpha}\mathbf{E}\left[\frac{-4r_i r_j}{\alpha}\right] - 2\frac{r_i^2 + r_j^2 + (z_k - z_l)^2}{\sqrt{\alpha}}\mathbf{K}\left[\frac{-4r_i r_j}{\alpha}\right] \\ \alpha &= (r_i - r_j)^2 + (z_k - z_l)^2 \end{aligned} \tag{16}$$

4. Study and characteristics of axial bearings with axially polarized ring magnets and a cylindrical air gap.

4.1 Structures with two ring magnets

This section considers devices constituted of two ring magnets with antiparallel polarization directions. So, the devices work as axial bearings. The influence of the different parameters of the geometry on both the axial force and stiffness is studied.

4.1.1 Geometry

The device geometry is shown on Fig.1. The radii remain the same as previously defined. Both ring magnets have the same axial dimension, the height $h_1 = h_2 = h$. The axial coordinate, z, characterizes the axial displacement of the inner ring with regard to the outer one. The polarization of the magnets is equal to $1T$.
The initial set of dimensions for each study is the following:
$r_1 = 25mm, r_2 = 28mm, r_3 = 21mm, r_4 = 24mm, h = 3mm$
Thus the initial air gap is $1mm$ wide and the ring magnets have an initial square cross section of $3 \times 3mm^2$.

4.1.2 Air gap influence

The ring cross section is kept constant and the radial dimension of the air gap, $r_1 - r_3$, is varied by modifying the radii of the inner ring. Fig.3 and 4 show how the axial force and stiffness are modified when the axial inner ring position changes for different values of the air gap.
Naturally, when the air gap decreases, the modulus of the axial force for a given axial position of the inner ring increases (except for large displacements) and so does the modulus of the axial stiffness. Furthermore, it has to be noted that a positive stiffness corresponds to a stable configuration in which the force is a pull-back one, whereas a negative stiffness corresponds to an unstable position: the inner ring gets ejected!

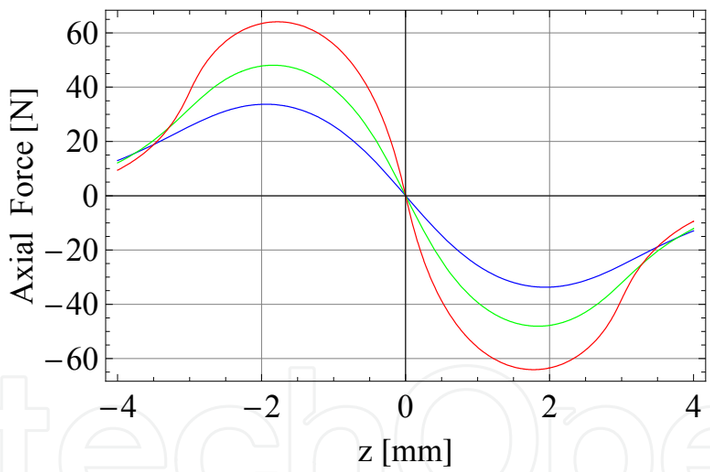

Fig. 3. Axial force for several air gap radial dimensions. Blue: $r_1 = 25mm, r_2 = 28mm, r_3 = 21mm, r_4 = 24mm, h = 3mm$ Air gap $1mm$, Green: Air gap $0.5mm$, Red: Air gap $0.1mm$

4.1.3 Ring height influence

The air gap is kept constant as well as the ring radii and the height of the rings is varied. Fig.5 and 6 show how the axial force and stiffness are modified. When the magnet height decreases, the modulus of the axial force for a given axial position of the inner ring decreases. This is normal, as the magnet volume also decreases.
The study of the stiffness is carried out for decreasing ring heights (Fig.6) but also for increasing ones (Fig.7). As a result, the stiffness doesn't go on increasing in a significant way above a given ring height. This means that increasing the magnet height, and consequently

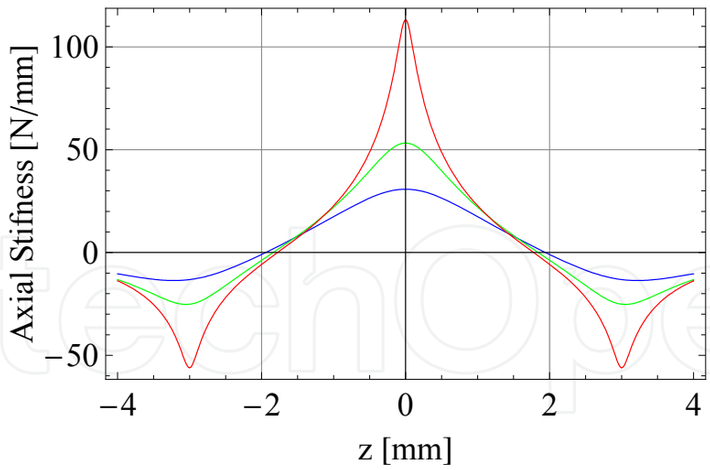

Fig. 4. Axial stiffness for several air gap radial dimensions. Blue: $r_1 = 25mm, r_2 = 28mm, r_3 = 21mm, r_4 = 24mm, h = 3mm$ Air gap $1mm$, Green: Air gap $0.5mm$, Red: Air gap $0.1mm$

the magnet volume, above a given value isn't interesting to increase the stiffness. Moreover, it has to be noted that when the height is reduced by half, from $3mm$ to $1.5mm$, the stiffness is only reduced by a third. This points out that in this configuration, the loss on the stiffness isn't that bad whereas the gain in volume is really interesting. This result will be useful for other kinds of bearing structures -stacked structures- in a further section. Besides, the magnet height shouln't become smaller than the half of its radial thickness unless the demagnetizing field inside the magnet becomes too strong and demagnetizes it.

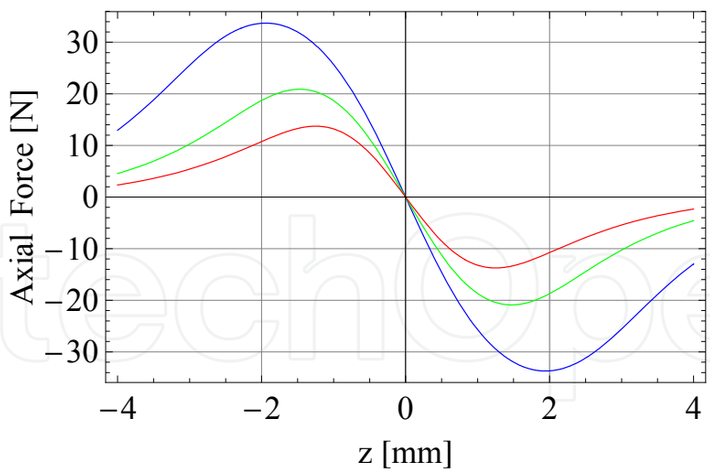

Fig. 5. Axial force for ring small heights. Blue: $r_1 = 25mm, r_2 = 28mm, r_3 = 21mm, r_4 = 24mm$, air gap $1mm$ $h = 3mm$, Green: $h = 2mm$, Red: $h = 1.5mm$.

4.1.4 Ring radial thickness influence

Now, the radial thickness of the ring magnets is varied. The ring height, $h = 3mm$, and the air gap length, $1mm$, are kept constant and the outer radius of the outer ring, r_2, is increased of

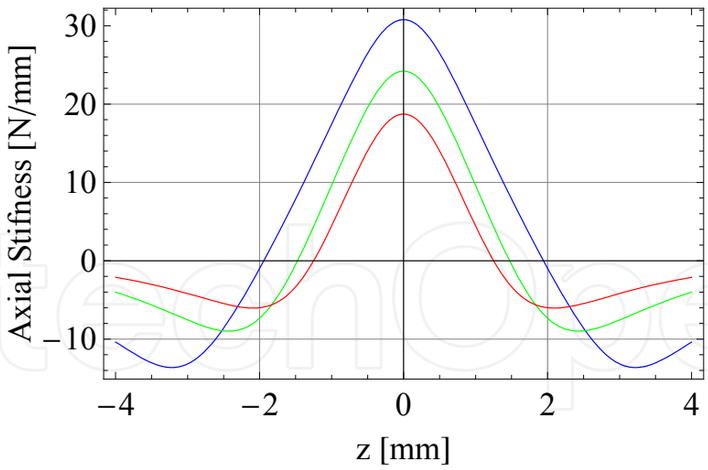

Fig. 6. Axial stiffness for ring small heights. Blue: $r_1 = 25mm, r_2 = 28mm, r_3 = 21mm, r_4 = 24mm$, air gap $1mm$ $h = 3mm$, Green: $h = 2mm$, Red: $h = 1.5mm$.

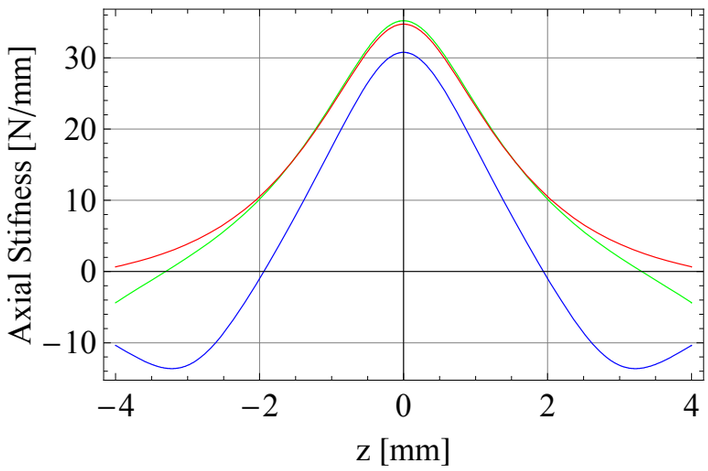

Fig. 7. Axial stiffness for ring large heights. Blue: $r_1 = 25mm, r_2 = 28mm, r_3 = 21mm, r_4 = 24mm$, air gap $1mm$ $h = 3mm$, Green: $h = 6mm$, Red: $h = 9mm$.

the same quantity as the inner radius of the inner ring, r_3, is decreased. So, the inner ring has always the same radial thickness as the outer one.
When the radial thickness increases, the modulus of the axial force for a given axial displacement of the inner ring also increases (Fig.8). This behavior is expected as once again the magnet volume increases. However, the ring thickness doesn't seem a very sensitive parameter. Indeed, the variation isn't as dramatic as with the previous studied parameters.

4.1.5 Ring mean perimeter influence

The outer ring perimeter is varied and all the radii are varied to keep the ring cross section and the air gap constant. As a result, when the device perimeter -or the air gap perimeter- increases, the modulus of the axial force for a given axial displacement of the inner ring also

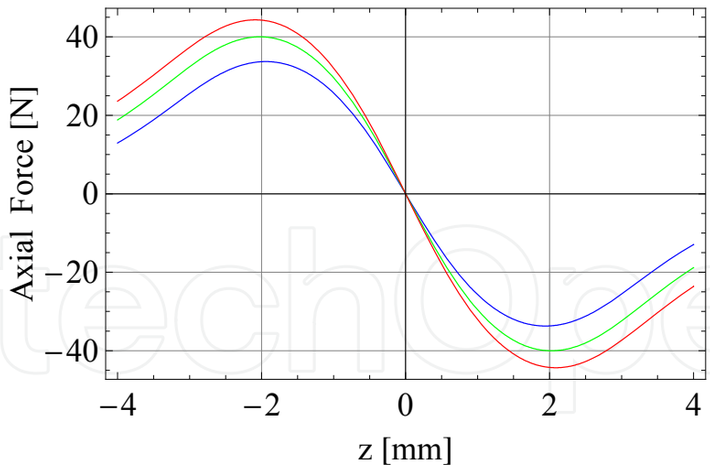

Fig. 8. Axial force for several radial thicknesses. Blue: $r_1 = 25mm, r_2 = 28mm, r_3 = 21mm, r_4 = 24mm$, $h = 3mm$, air gap $1mm$, Radial thickness $r_2 - r_1 = r_4 - r_3 = 3mm$, Green: $4mm$, Red: $5mm$.

increases (Fig.9). This result is expected as the magnet volume also increases.

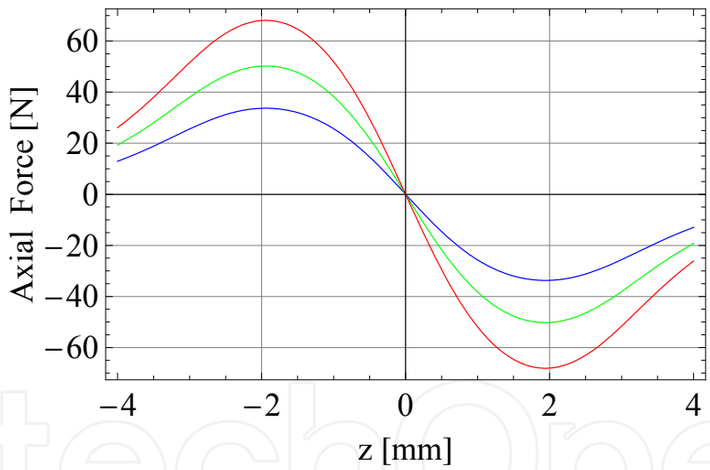

Fig. 9. Axial force for several air gap perimeters. $h = 3mm$, air gap $1mm$. Blue: $r_1 = 25mm, r_2 = 28mm, r_3 = 21mm, r_4 = 24mm$. Green: $r_1 = 37mm, r_2 = 40mm, r_3 = 33mm, r_4 = 36mm$. Red: $r_1 = 50mm, r_2 = 53mm, r_3 = 46mm, r_4 = 49mm$.

4.1.6 Maximum axial force

Previous results are interesting as they show the shape of the axial force and stiffness when different dimensional parameters are varied. Nevertheless, it is necessary to complete these results with additional studies, such as the study of the maximum force for example, in order to compare them. Indeed, a general conclusion is that the axial force increases when the magnet volume increases, but the way it increases depends on the parameter which makes the volume increase.

So, the blue line on Fig.10 shows that the maximum force varies linearly with the air gap diameter. Furthermore, this variation is also linear for radially thicker ring magnets (green and red lines on Fig.10).
As a conclusion, the maximum axial force, and the axial stiffness too, is proportional to the air gap diameter, as long as this diameter isn't too small (which means above 5mm).

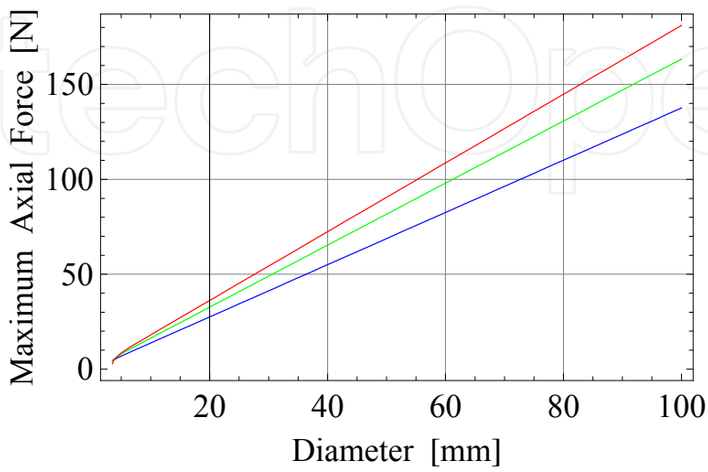

Fig. 10. Maximum axial force versus the air gap perimeter for several ring radial thicknesses. Air gap $1mm$, $h = 3mm$. Blue: $r_1 = 25mm, r_2 = 28mm, r_3 = 21mm, r_4 = 24mm$ Radial thickness $r_2 - r_1 = r_4 - r_3 = 3mm$, Green: Radial thickness $4mm$, Red: Radial thickness $5mm$.

Moreover, the blue line on Fig.11 shows that the maximum force varies inversely to the square of the air gap radial dimension. Thus, the maximum axial force is very sensitive to the air gap radial dimension, which should be as small as possible to have large forces but which is generally set by the mechanical constraints of the device. As a remark, for ring magnets of $3 \times 3mm^2$ cross section, if the radial mechanical air gap has to be $2mm$, the axial force exerted is rather negligible!

4.2 Multiple ring structures: stacked structures

A remark of the previous section will be exploited now. Indeed, the study of the ring height shew that diminishing the magnet height, and thus its volume, could be done without a dramatical decrease of the force. Hence the idea of using rather short rings but of stacking them with alternate polarization directions to achieve larger forces.
For example, let's consider a stack of elementary devices of same dimensions as the previously considered devices: $r_1 = 25mm$, $r_2 = 28mm$, $r_3 = 21mm$, $r_4 = 24mm$, $h = 3mm$, cross section $3 \times 3mm^2$. The bottom of the first device is located at $z = 0$, the bottom of the second one at $z = 3$ and so on (Fig. 12).
Fig.13 shows the axial stiffness for the elementary device (blue), for a stack of two elementary devices (green) and for a stack of three elementary devices (red). The consequence of stacking is that the different axial stiffnesses are additive, as they all act in the same way. So, the total axial stiffness of the device increases more rapidly than the number of stacked devices (Yonnet et al., 1991). Indeed, the maximal stiffness for one ring pair with a square section of $3 \times 3mm^2$ is 30.8 N/mm, for two pairs 87.9 N/mm and for three pairs 140 N/mm. If n is the number of pairs, the stiffness of a stack is approximately $2n - 1$ times greater than the stiffness of a pair.

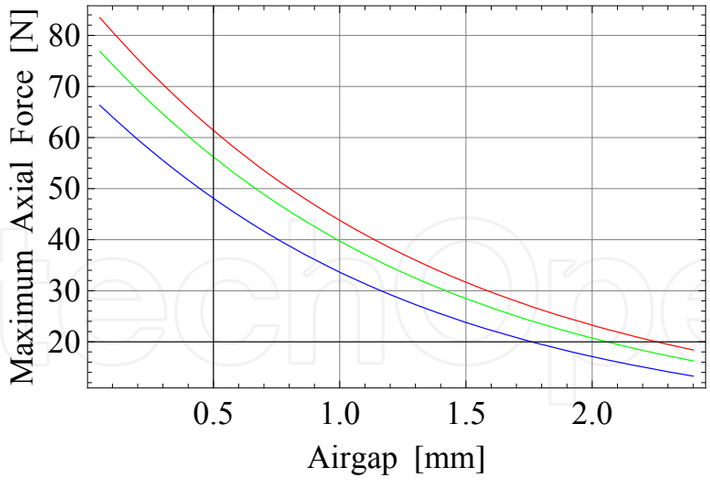

Fig. 11. Maximum axial force versus the air gap radial dimension for several ring radial thicknesses. $h = 3mm$. Blue: $r_1 = 25mm, r_2 = 28mm, r_3 = 21mm, r_4 = 24mm$ Radial thickness $r_2 - r_1 = r_4 - r_3 = 3mm$, Green: Radial thickness $4mm$, Red: Radial thickness $5mm$.

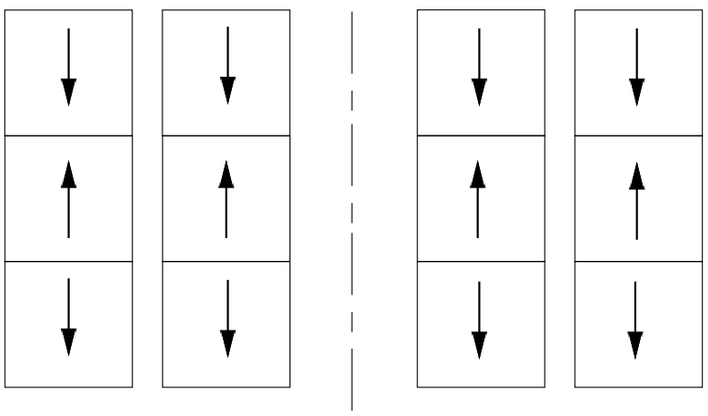

Fig. 12. Cross-section of a stack of three elementary devices with alternate axial polarizations.

Besides, the stiffness obtained for a ring pair of same total dimensions as the stack of three pairs is 34.7 N/mm. This example emphazises the advantage, for a given volume and a sufficient axial height, of splitting the ring into several rings of smaller heights and opposite polarizations: making three pairs increases the stiffness fourfold. The splitting is interesting as long as the height of each ring magnet is large enough (see section 4.1.3).

5. Study and characteristics of axial bearings with axially polarized ring magnets and a plane air gap.

This section considers devices with two axially polarized ring magnets of exactly the same dimensions. They are positioned so as to have the same rotation axis and thus are separated by a plane air gap. In this configuration, if the rings have the same polarization direction, the device works as a radial bearing, if the polarizations are opposite, it works as an axial bearing. It is noticeable that for axial polarizations, parallel polarizations yield

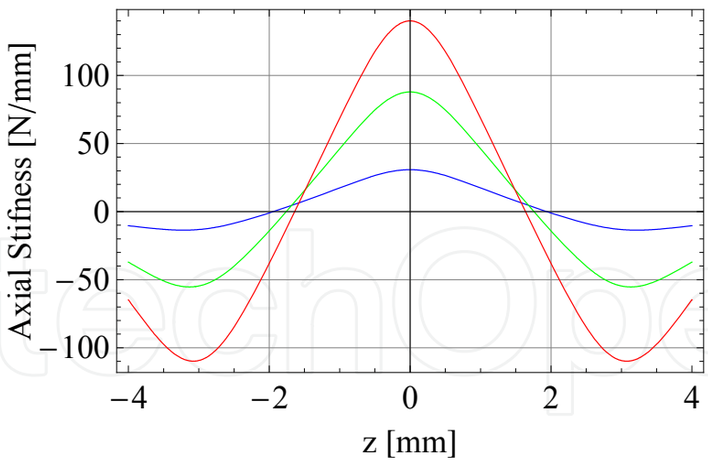

Fig. 13. Axial stiffness for one elementary device (blue), for a stack of two elementary devices (green) and three elementary devices (red).

radial bearings whereas antiparallel polarizations yield axial ones, whatever the air gap shape.

For these structures, the axial displacement of one ring corresponds to an air gap variation. Of course, the maximal axial force between the rings occurs when they are axially in contact with each other. When the air gap, z, increases, the axial force decreases, as show on Fig.15. As the variation is monotonous, the axial stiffness has always the same sign (Fig. 16) and the force the same nature (restoring, here).

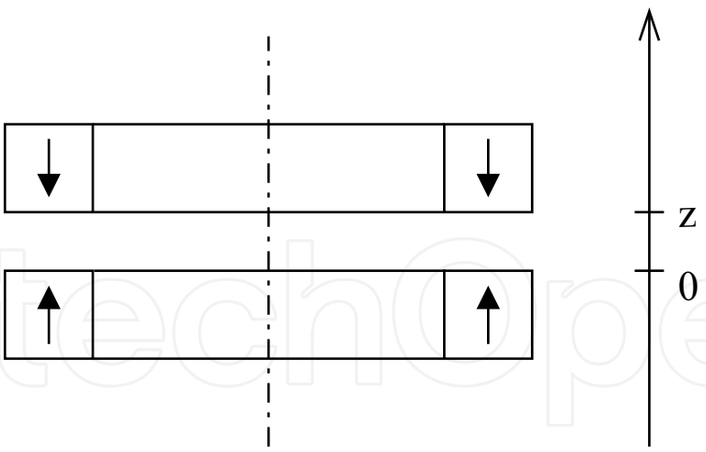

Fig. 14. Cross-section of a bearing with a plane air gap

Moreover, the axial force depends on the size of surfaces which are facing each other. Therefore, it is obvious that when the ring radial thickness increases, the force increases in the same way. The only other interesting parameter is the ring axial height. Figure 17 and 18 show how the axial force and stiffness vary when the air gap changes for different ring axial height. The force doesn't seem to vary greatly when the magnet height changes, and the stiffness even less. But the attention should be drawn to the scale of the force amplitude. Indeed, Fig.19 and 20 show the force and the stiffness for a fixed air gap when the magnet height varies.

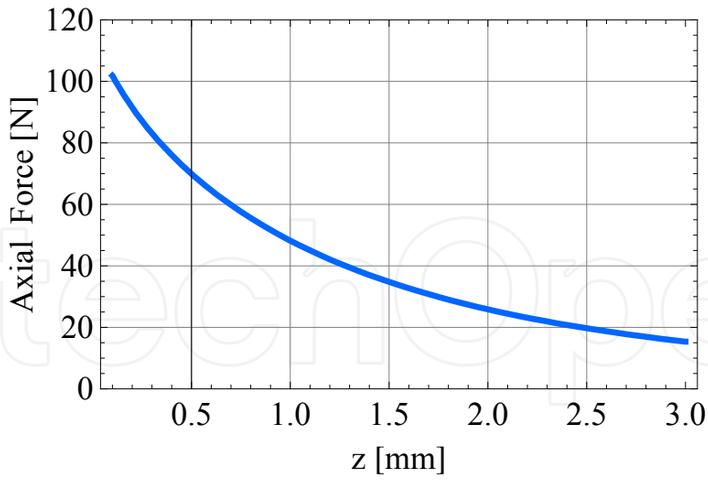

Fig. 15. Axial force when the plane air gap length, z, varies. $r_1 = r_3 = 25mm, r_2 = r_4 = 28mm, h = 3mm$.

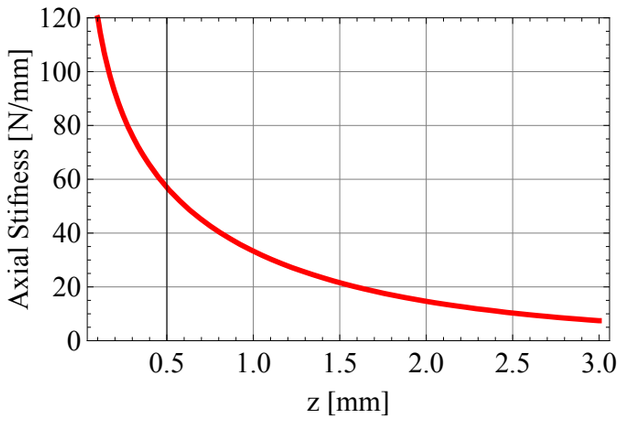

Fig. 16. Axial stiffness when the plane air gap length, z, varies. $r_1 = r_3 = 25mm, r_2 = r_4 = 28mm, h = 3mm$.

They emphazise the fact that increasing the magnet height is interesting for small heights, but becomes rapidly inefficient, especially with regard to the stiffness.

6. Determination of the force transmitted between two radially polarized ring permanent magnets.

The structure considered now is shown in Fig 21. The device is constituted by two concentric ring magnets which are separated by a cylindrical air gap and are radially polarized, their polarizations being in the same direction.

6.1 Notations

The parameters which describe the geometry of Fig.21 and its properties are listed below:
J_1: outer ring polarization [T].
J_2: inner ring polarization [T].

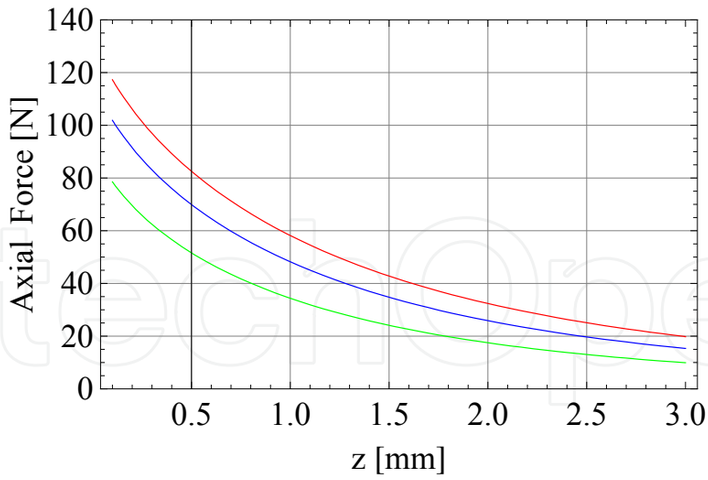

Fig. 17. Axial force when the plane air gap length, z, varies. $r_1 = r_3 = 25mm$, $r_2 = r_4 = 28mm$. Blue: $h = 3mm$, Green: $h = 2mm$, Red: $h = 4mm$.

r_{in}, r_{out}: radial coordinates of the outer ring [m].
r_{in2}, r_{out2}: radial coordinates of the inner ring [m].
h: outer ring height [m].
$z_b - z_a$: inner ring height [m].
The rings are radially centered and their polarizations are supposed to be uniformly radial.

6.2 Magnet modelling

For this kind of configuration, the coulombian model of magnets is the one that gives interesting analytical and semi analytical expressions. Consequently, each ring permanent magnet is represented by two curved planes which correspond to the inner and outer faces of the rings. These faces are charged with a surface magnetic pole density σ^* and the charge balance is reached thanks to a magnetic pole volume density σ_v^*. For each ring, the inner face is charged with the surface magnetic pole density $+\sigma^*$ and the outer one is charged with the surface magnetic pole density $-\sigma^*$. Moreover, all the calculations are carried out with $\sigma^* = \vec{J}.\vec{n} = 1T$ where $\vec{J}$ is the magnetic polarization vector and $\vec{n}$ is the unit normal vector which is directed towards the rotation axis.

6.3 Expression of the force

The axial force exerted between the magnets results of the interaction of all the charge densities. The axial component of the magnetic field produced by the outer ring permanent magnet is H_z. Thus, the axial force F_z can be written as follows:

$$F_z = \int\int_{(S_{in})} H_z \sigma_2^* d\tilde{S} - \int\int_{(S_{out})} H_z \sigma_2^* d\tilde{S} + \int\int\int_{(V)} H_z \frac{\sigma_2^*}{r_2} d\tilde{V} \tag{17}$$

where σ_2^* is the magnetic pole surface density of the inner ring magnet, (S_{in}) is the surface of the inner face of the inner ring permanent magnet, (S_{out}) is the surface of the outer face of the inner ring permanent magnet and (V) is the volume of the inner ring permanent magnet. So,

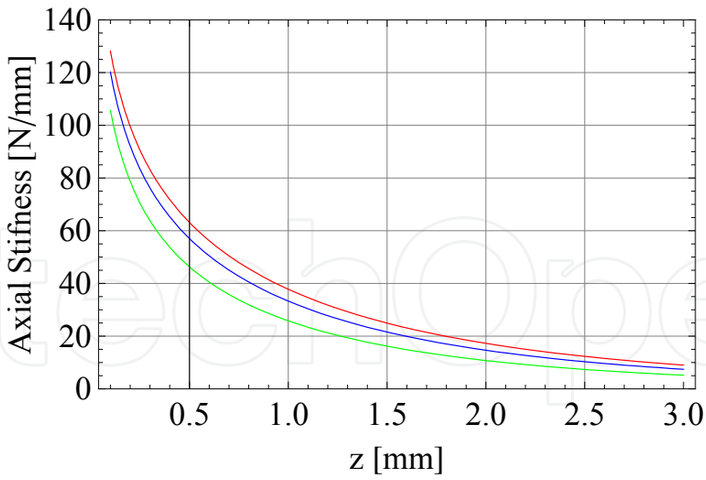

Fig. 18. Axial stiffness when the plane air gap length, z, varies. $r_1 = r_3 = 25mm$,$r_2 = r_4 = 28mm$. Blue: $h = 3mm$, Green: $h = 2mm$, Red: $h = 4mm$.

the axial force F_z can be expressed by:

$$\begin{aligned}
F_z \quad = \quad & -\int_{\theta_1=0}^{2\pi}\int_{z_1=0}^{h}\int_{\theta_2=0}^{2\pi}\int_{z_2=z_a}^{z_b} a(r_{in}, r_{out2})dz_1 d\theta_1 dz_2 d\theta_2 \\
& +\int_{\theta_1=0}^{2\pi}\int_{z_1=0}^{h}\int_{\theta_2=0}^{2\pi}\int_{z_2=z_a}^{z_b} a(r_{out}, r_{out2})dz_1 d\theta_1 dz_2 d\theta_2 \\
& +\int_{\theta_1=0}^{2\pi}\int_{z_1=0}^{h}\int_{\theta_2=0}^{2\pi}\int_{z_2=z_a}^{z_b} a(r_{in}, r_{in2})dz_1 d\theta_1 dz_2 d\theta_2 \\
& -\int_{\theta_1=0}^{2\pi}\int_{z_1=0}^{h}\int_{\theta_2=0}^{2\pi}\int_{z_2=z_a}^{z_b} a(r_{out}, r_{in2})dz_1 d\theta_1 dz_2 d\theta_2 \\
& -\int_{r_1=r_{in}}^{r_{out}}\int_{\theta_1=0}^{2\pi}\int_{z_1=0}^{h}\int_{\theta_2=0}^{2\pi}\int_{z_2=z_a}^{z_b} b(r_{out2}, r_1)dr_1 dz_1 d\theta_1 dz_2 d\theta_2 \\
& +\int_{r_1=r_{in}}^{r_{out}}\int_{\theta_1=0}^{2\pi}\int_{z_1=0}^{h}\int_{\theta_2=0}^{2\pi}\int_{z_2=z_a}^{z_b} b(r_{in2}, r_1)dr_1 dz_1 d\theta_1 dz_2 d\theta_2 \\
& +\int_{r_2=r_{in2}}^{r_{out2}}\int_{\theta_1=0}^{2\pi}\int_{z_1=0}^{h}\int_{\theta_2=0}^{2\pi}\int_{z_2=z_a}^{z_b} b(r_{in}, r_2)dz_1 d\theta_1 dr_2 dz_2 d\theta_2 \\
& -\int_{r_2=r_{in2}}^{r_{out2}}\int_{\theta_1=0}^{2\pi}\int_{z_1=0}^{h}\int_{\theta_2=0}^{2\pi}\int_{z_2=z_a}^{z_b} b(r_{out}, r_2)dz_1 d\theta_1 dr_2 dz_2 d\theta_2 \\
& +\int_{r_1=r_{in}}^{r_{out}}\int_{r_2=r_{in2}}^{r_{out2}}\int_{\theta_1=0}^{2\pi}\int_{z_1=0}^{h}\int_{\theta_2=0}^{2\pi}\int_{z_2=z_a}^{z_b} c(r_1, r_2)dr_1 dz_1 d\theta_1 dr_2 dz_2 d\theta_2
\end{aligned} \tag{18}$$

with

$$a(\alpha, \beta) = \frac{\sigma_1^* \sigma_2^*}{4\pi\mu_0} \frac{(z_2 - z_1)\alpha\beta}{(\alpha^2 + \beta^2 - 2\alpha\beta + (z_2 - z_1)^2)^{\frac{3}{2}}} \tag{19}$$

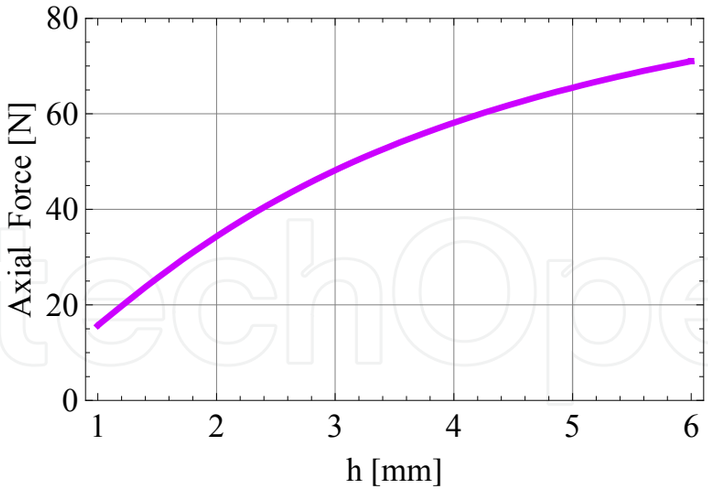

Fig. 19. Axial force when the ring axial height, h, varies. Plane air gap $z = 1mm$, $r_1 = r_3 = 25mm$, $r_2 = r_4 = 28mm$.

where σ_1^* is the magnetic pole surface density of the outer ring magnet. and

$$b(\alpha,\beta) = \frac{a(\alpha,\beta)}{\beta} \tag{20}$$

$$c(\alpha,\beta) = \frac{a(\alpha,\beta)}{\alpha\beta} \tag{21}$$

The next step is to evaluate Eq. (18). Therefore, the number of integrals is first reduced by integrating analytically $a(\alpha,\beta)$, $b(\alpha,\beta)$ and $c(\alpha,\beta)$ according to the integral variables. Unfortunately, a fully analytical expression of the force can't be found but the following semi-analytical expression is quite useful:

$$\begin{aligned} F_z &= \frac{\sigma_1^*\sigma_2^*}{2\mu_0}\int_{\theta_1=0}^{2\pi} S d\theta_1 \\ &+ \frac{\sigma_1^*\sigma_2^*}{2\mu_0}\int_{\theta_1=0}^{2\pi} M d\theta_1 \\ &+ \frac{\sigma_1^*\sigma_2^*}{2\mu_0}\int_{\theta_1=0}^{2\pi}\int_{r_2=r_{in2}}^{r_{out2}} V d\theta_1 dr_2 \end{aligned} \tag{22}$$

where S represents the interaction between the magnetic pole surface densities of each ring magnet, M corresponds to the magnetic interaction between the magnetic pole surface densities of one ring permanent magnet and the magnetic pole volume density of the other one, and V denotes the interaction between the magnetic pole volume densities of each ring permanent magnet.

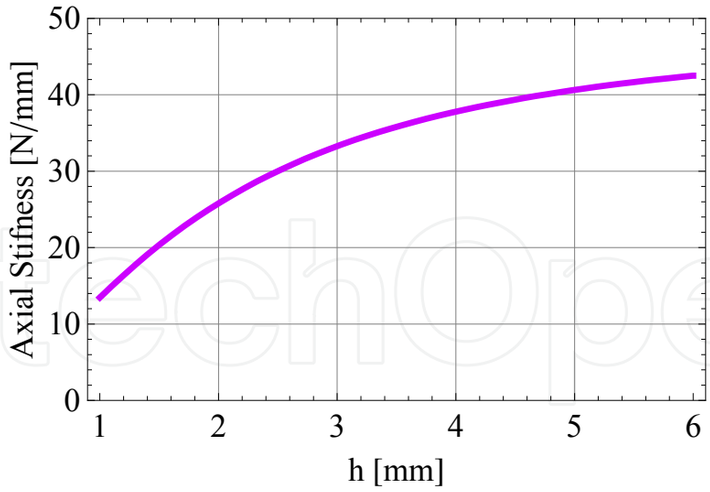

Fig. 20. Axial stiffness when the ring axial height, h, varies. Plane air gap $z = 1mm$, $r_1 = r_3 = 25mm$,$r_2 = r_4 = 28mm$.

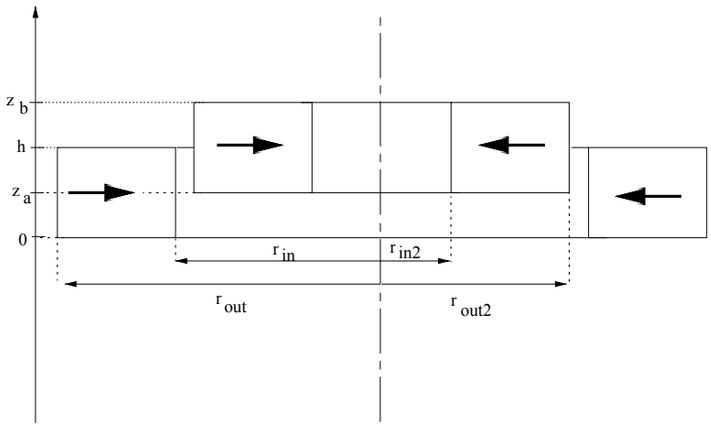

Fig. 21. Radial bearing with radially polarized ring magnets and a cylindrical air gap

The first contribution S is given by (23).

$$\begin{aligned} S &= -f(z_a, z_b, h, \theta_1, r_{in}, r_{out2}) \\ &\quad +f(z_a, z_b, h, \theta_1, r_{out}, r_{out2}) \\ &\quad +f(z_a, z_b, h, \theta_1, r_{in}, r_{in2}) \\ &\quad -f(z_a, z_b, h, \theta_1, r_{out}, r_{in2}) \end{aligned} \tag{23}$$

with

$$\begin{aligned} f(\alpha_1,\alpha_2,\alpha_3,\theta_1,\alpha_5,\alpha_6) &= \alpha_5\alpha_6 \log\left[\alpha_3-\alpha_1+\sqrt{\alpha_5^2+\alpha_6^2+(\alpha_3-\alpha_1)^2-2\alpha_5\alpha_6\cos(\theta_1)}\right] \\ &+\alpha_5\alpha_6 \log\left[\alpha_1+\sqrt{\alpha_5^2+\alpha_6^2+\alpha_1^2-2\alpha_5\alpha_6\cos(\theta_1)}\right] \\ &-\alpha_5\alpha_6 \log\left[\alpha_3-\alpha_2+\sqrt{\alpha_5^2+\alpha_6^2+(\alpha_3-\alpha_2)^2-2\alpha_5\alpha_6\cos(\theta_1)}\right] \\ &-\alpha_5\alpha_6 \log\left[\alpha_2+\sqrt{\alpha_5^2+\alpha_6^2+\alpha_2^2-2\alpha_5\alpha_6\cos(\theta_1)}\right] \end{aligned} \tag{24}$$

The second contribution M is given by (25).

$$\begin{aligned} M &= -t(r_{in},r_{out},r_{out2},h,z_a,z_b,\theta_1) \\ &+t(r_{in},r_{out},r_{in2},h,z_a,z_b,\theta_1) \\ &+t(r_{in},r_{out},r_{in},h,z_a,z_b,\theta_1) \\ &-t(r_{in},r_{out},r_{out},h,z_a,z_b,\theta_1) \end{aligned} \tag{25}$$

with

$$\begin{aligned} t(\beta_1,\beta_2,\beta_3,\beta_4,\beta_5,\beta_6,\theta_1) &= t^{(2)}\left(\beta_1,\beta_2,\beta_4-\beta_5,\beta_3^2+(\beta_4-\beta_5)^2,2\beta_3\cos(\theta_1)\right) \\ &+t^{(2)}\left(\beta_1,\beta_2,\beta_5,\beta_3^2+\beta_5^2,2\beta_3\cos(\theta_1)\right) \\ &-t^{(2)}\left(\beta_1,\beta_2,\beta_4-\beta_6,\beta_3^2+(\beta_4-\beta_6)^2,2\beta_3\cos(\theta_1)\right) \\ &-t^{(2)}\left(\beta_1,\beta_2,\beta_6,\beta_3^2+\beta_6^2,2\beta_3\cos(\theta_1)\right) \end{aligned} \tag{26}$$

and

$$t^{(2)}(\beta_1,\beta_2,q,d,f) = t^{(3)}(\beta_2,q,d,f) - t^{(3)}(\beta_1,q,d,f) \tag{27}$$

and

$$\begin{aligned} t^{(3)}(s,q,d,f) &= -s+\frac{\sqrt{4d-f^2-4q^2}}{2}\arctan\left[\frac{-f+2s}{\sqrt{4d-f^2-4q^2}}\right]-\frac{f}{4}\log\left[d-q^2-fs+s^2\right] \\ &+s\log\left[q+\sqrt{d-fs+s^2}\right]+q\log\left[-f+2(s+\sqrt{d-fs+s^2})\right] \\ &-\frac{\left(4d-f^2-4q^2+f\eta\right)\log\left[u_1\right]}{4\eta} \\ &-\frac{\left(-4d+f^2+4q^2+f\eta\right)\log\left[u_2\right]}{4\eta} \end{aligned} \tag{28}$$

$$\begin{aligned} u_1 &= -\frac{2\left(f^2+4fq^2-f^2(\eta+2s)+4d(-f+\eta+2s)\right)}{q^2(-4d+f^2+4q^2-f\eta)(-f+\eta+2s)} \\ &\quad -\frac{8q(-2qs+\eta\sqrt{d-fs+s^2})}{q^2(-4d+f^2+4q^2-f\eta)(-f+\eta+2s)} \end{aligned} \tag{29}$$

$$\begin{aligned} u_2 &= -\frac{2\left(f^2+4fq^2-f^2(\eta-2s)-4d(f+\eta-2s)\right)}{q^2(-4d+f^2+4q^2+f\eta)(f+\eta-2s)} \\ &\quad -\frac{-8q(2qs+\eta\sqrt{d-fs+s^2})}{q^2(-4d+f^2+4q^2+f\eta)(f+\eta-2s)} \end{aligned} \tag{30}$$

with

$$\eta = \sqrt{-4d+f^2+4q^2} \tag{31}$$

The third contribution V is given by (32).

$$V = th^{(1)}(r_{out}, r_2, z_a, z_b, h, \theta_1) - th^{(1)}(r_{in}, r_2, z_a, z_b, h, \theta_1) \tag{32}$$

with

$$\begin{aligned} th^{(1)} &= t^{(3)}(r_1, h-z_a, r_2^2+(h-z_a)^2, 2r_2\cos(\theta_1)) \\ &\quad +t^{(3)}(r_1, z_a, r_2^2+z_a^2, 2r_2\cos(\theta_1)) \\ &\quad -t^{(3)}(r_1, h-z_b, r_2^2+(h-z_b)^2, 2r_2\cos(\theta_1)) \\ &\quad -t^{(3)}(r_1, z_b, r_2^2+z_b^2, 2r_2\cos(\theta_1)) \end{aligned} \tag{33}$$

6.4 Expression of the axial stiffness between two radially polarized ring magnets

As previously done, the stiffness K exerted between two ring permanent magnets is determined by calculating the derivative of the axial force with respect to z_a. We set $z_b = z_a + b$ where b is the height of the inner ring permanent magnet. Thus, the axial stiffness K can be calculated with (34).

$$K = -\frac{\partial}{\partial z_a} F_z \tag{34}$$

where F_z is given by (18). We obtain :

$$K = K_S + K_M + K_V \tag{35}$$

where K_S represents the stiffness determined by considering only the magnetic pole surface densities of each ring permanent magnet, K_M corresponds to the stiffness determined with the interaction between the magnetic pole surface densities of one ring permanent magnet and the magnetic pole volume density of the other one, and K_V corresponds to the stiffness determined with the interaction between the magnetic pole volume densities of each ring permanent magnet. Thus, K_S is given by:

$$K_S =$$

$$\begin{aligned}
&\eta_{31}\left(\frac{1}{\sqrt{\alpha_{31}}}\mathbf{K}^*\left[-\frac{4r_3r_1}{\alpha_{31}}\right]-\frac{1}{\sqrt{\beta_{31}}}\mathbf{K}^*\left[-\frac{4r_3r_1}{\beta_{31}}\right]+\frac{1}{\sqrt{\delta_{31}}}\mathbf{K}^*\left[-\frac{4r_3r_1}{\delta_{31}}\right]-\frac{1}{\sqrt{\gamma_{31}}}\mathbf{K}^*\left[-\frac{4r_3r_1}{\gamma_{31}}\right]\right)\\
&+\eta_{41}\left(\frac{1}{\sqrt{\alpha_{41}}}\mathbf{K}^*\left[-\frac{4r_4r_1}{\alpha_{41}}\right]-\frac{1}{\sqrt{\beta_{41}}}\mathbf{K}^*\left[-\frac{4r_4r_1}{\beta_{41}}\right]+\frac{1}{\sqrt{\delta_{41}}}\mathbf{K}^*\left[-\frac{4r_4r_1}{\delta_{41}}\right]-\frac{1}{\sqrt{\gamma_{41}}}\mathbf{K}^*\left[-\frac{4r_4r_1}{\gamma_{41}}\right]\right)\\
&+\eta_{32}\left(\frac{1}{\sqrt{\alpha_{32}}}\mathbf{K}^*\left[-\frac{4r_3r_2}{\alpha_{32}}\right]-\frac{1}{\sqrt{\beta_{32}}}\mathbf{K}^*\left[-\frac{4r_3r_2}{\beta_{32}}\right]+\frac{1}{\sqrt{\delta_{32}}}\mathbf{K}^*\left[-\frac{4r_3r_2}{\delta_{32}}\right]-\frac{1}{\sqrt{\gamma_{32}}}\mathbf{K}^*\left[-\frac{4r_3r_2}{\gamma_{32}}\right]\right)\\
&+\eta_{42}\left(\frac{1}{\sqrt{\alpha_{42}}}\mathbf{K}^*\left[-\frac{4r_4r_2}{\alpha_{42}}\right]-\frac{1}{\sqrt{\beta_{42}}}\mathbf{K}^*\left[-\frac{4r_4r_2}{\beta_{42}}\right]+\frac{1}{\sqrt{\delta_{42}}}\mathbf{K}^*\left[-\frac{4r_4r_2}{\delta_{42}}\right]-\frac{1}{\sqrt{\gamma_{42}}}\mathbf{K}^*\left[-\frac{4r_4r_2}{\gamma_{42}}\right]\right)
\end{aligned} \tag{36}$$

with

$$\eta_{ij} = \frac{2r_ir_j\sigma^*}{\mu_0} \tag{37}$$

$$\alpha_{ij} = (r_i - r_j)^2 + z_a^2 \tag{38}$$

$$\beta_{ij} = (r_i - r_j)^2 + (z_a + h)^2 \tag{39}$$

$$\gamma_{ij} = (r_i - r_j)^2 + (z_a - h) \tag{40}$$

$$\delta_{ij} = (r_i - r_j)^2 + (b - h)^2 + z_a(2b - 2h + z_a) \tag{41}$$

$$\mathbf{K}^*[m] = \int_0^{\frac{\pi}{2}} \frac{1}{\sqrt{1 - m\sin(\theta)^2}} d\theta \tag{42}$$

The second contribution K_M is given by:

$$K_M = \frac{\sigma_1^*\sigma_2^*}{2\mu_0}\int_{\theta=0}^{2\pi} u d\theta \tag{43}$$

with

$$\begin{aligned}
u \quad = \quad & f(r_{in}, r_{out}, r_{in2}, h, z_a, b, \theta)\\
& -f(r_{in}, r_{out}, r_{out2}, h, z_a, b, \theta)\\
& +f(r_{in2}, r_{out2}, r_{in}, h, z_a, b, \theta)\\
& -f(r_{in2}, r_{out2}, r_{out}, h, z_a, b, \theta)
\end{aligned} \tag{44}$$

and

$$
\begin{aligned}
f(\alpha,\beta,\gamma,h,z_a,b,\theta) = \\
&-\gamma\log\left[\alpha-\gamma\cos(\theta)+\sqrt{\alpha^2+\gamma^2+z_a^2-2\alpha\gamma\cos(\theta)}\right] \\
&+\gamma\log\left[\alpha-\gamma\cos(\theta)+\sqrt{\alpha^2+\gamma^2+(z_a+b)^2-2\alpha\gamma\cos(\theta)}\right] \\
&+\gamma\log\left[\alpha-\gamma\cos(\theta)+\sqrt{\alpha^2+\gamma^2+(z_a-h)^2-2\alpha\gamma\cos(\theta)}\right] \\
&-\gamma\log\left[\alpha-\gamma\cos(\theta)+\sqrt{\alpha^2+\gamma^2+(b-h)^2+2z_a(b-h)+z_a^2-2\alpha\gamma\cos(\theta)}\right] \\
&+\gamma\log\left[\beta-\gamma\cos(\theta)+\sqrt{\beta^2+\gamma^2+z_a^2-2\alpha\gamma\cos(\theta)}\right] \\
&-\gamma\log\left[\beta-\gamma\cos(\theta)+\sqrt{\beta^2+\gamma^2+(z_a+b)^2-2\alpha\gamma\cos(\theta)}\right] \\
&+\gamma\log\left[\beta-\gamma\cos(\theta)+\sqrt{\beta^2+\gamma^2+(z_a-h)^2-2\alpha\gamma\cos(\theta)}\right] \\
&-\gamma\log\left[\beta-\gamma\cos(\theta)+\sqrt{\beta^2+\gamma^2+(b-h)^2+2z_a(b-h)+z_a^2-2\alpha\gamma\cos(\theta)}\right]
\end{aligned}
\tag{45}
$$

The third contribution K_V is given by:

$$
K_V = \frac{\sigma_1^*\sigma_2^*}{2\mu_0}\int_{\theta=0}^{2\pi}\int_{r_1=r_{in}}^{r_{out}}\delta d\theta \tag{46}
$$

with

$$
\begin{aligned}
\delta \quad = \quad & -\log\left[r_{in2}-r_1\cos(\theta)+\sqrt{r_1^2+r_{in2}^2+z_a^2-2r_1r_{in2}\cos(\theta)}\right] \\
&+\log\left[r_{in2}-r_1\cos(\theta)+\sqrt{r_1^2+r_{in2}^2+(z_a+b)^2-2r_1r_{in2}\cos(\theta)}\right] \\
&-\log\left[r_{in2}-r_1\cos(\theta)+\sqrt{r_1^2+r_{in2}^2+(b-h)^2+2bz_a-2hz_a+z_a^2-2r_1r_{in2}\cos(\theta)}\right] \\
&+\log\left[r_{in2}-r_1\cos(\theta)+\sqrt{r_1^2+r_{in2}^2+(z_a-h)^2-2r_1r_{in2}\cos(\theta)}\right] \\
&+\log\left[r_{out2}-r_1\cos(\theta)+\sqrt{r_1^2+r_{out2}^2+z_a^2-2r_1r_{out2}\cos(\theta)}\right] \\
&-\log\left[r_{out2}-r_1\cos(\theta)+\sqrt{r_1^2+r_{out2}^2+(z_a+b)^2-2r_1r_{out2}\cos(\theta)}\right] \\
&-\log\left[r_{out2}-r_1\cos(\theta)+\sqrt{r_1^2+r_{out2}^2+(z_a-h)^2-2r_1r_{out2}\cos(\theta)}\right] \\
&+\log\left[r_{out2}-r_1\cos(\theta)+\sqrt{r_1^2+r_{out2}^2+(b-h)^2+2bz_a-2hz_a+z_a^2-2r_1r_{out2}\cos(\theta)}\right]
\end{aligned}
\tag{47}
$$

As a remark, the expression of the axial stiffness can be determined analytically if the magnetic pole surface densities of each ring only are taken into account, so, if the magnetic pole volume

densities can be neglected. This is possible when the radii of the ring permanent magnets are large enough (Ravaud, Lemarquand, Lemarquand & Depollier, 2009).

7. Study and characteristics of bearings with radially polarized ring magnets.

Radially polarized ring magnets can be used to realize passive bearings, either with a cylindrical air gap or with a plane one. A device with a cylindrical air gap works as an axial bearing when the ring magnets have the same radial polarization direction, whereas it works as a radial one for opposite radial polarizations.
For rings with a square cross-section and radii large enough to neglect the magnetic pole volume densities, the authors shew that the axial force exerted between the magnets as well as the corresponding siffness was the same whatever the polarization direction, axial or radial. For instance, this is illustrated for a radial bearing of following dimensions: $r_{in2} = 0.01$ m, $r_{out2} = 0.02$ m, $r_{in} = 0.03$ m, $r_{out} = 0.04$ m, $z_b - z_a = h = 0.1$ m, $J = 1$ T.
Fig. 22 gives the results obtained for a bearing with radial polarization. These results are to be compared with the ones of Fig. 23 corresponding to axial polarizations.

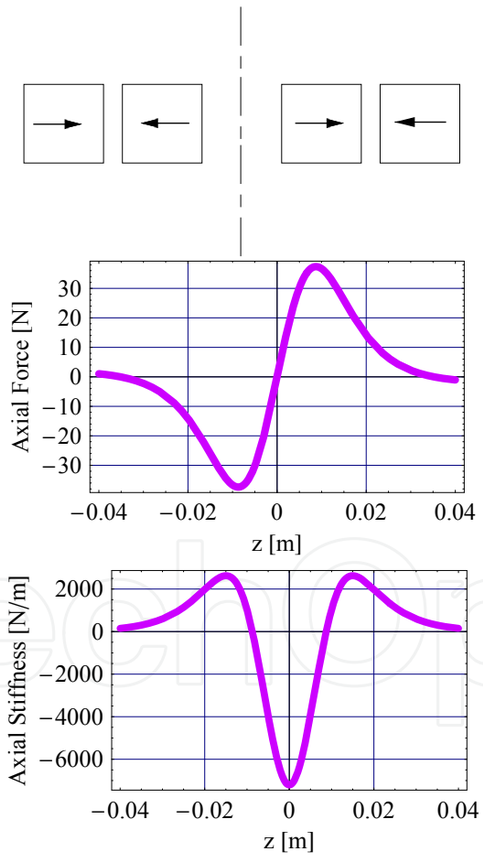

Fig. 22. Axial force and stiffness versus axial displacement for two ring permanent magnets with radial polarizations; $r_1 = 0.01$ m, $r_2 = 0.02$ m, $r_3 = 0.03$ m, $r_4 = 0.04$ m, $z_2 - z_1 = z_4 - z_3 = 0.1$ m, $J = 1$ T

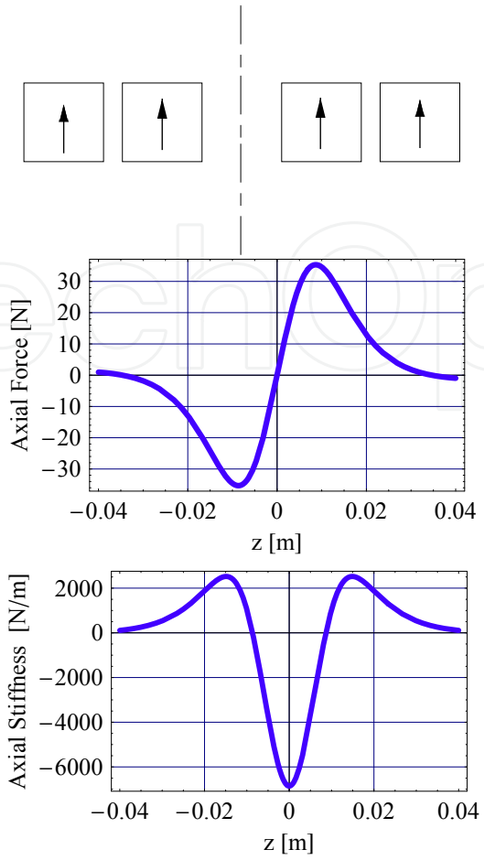

Fig. 23. Axial force and stiffness versus axial displacement for two ring permanent magnets with axial polarizations; $r_1 = 0.01$ m, $r_2 = 0.02$ m, $r_3 = 0.03$ m, $r_4 = 0.04$ m, $z_2 - z_1 = z_4 - z_3 = 0.1$ m, $J = 1$ T

These figures show clearly that the performances are the same. Indeed, for the radial polarizations the maximal axial force exerted by the outer ring on the inner one is 37.4 N and the maximal axial stiffness is $|K_z| = 7205$ N/m and for the axial polarizations the maximal axial force exerted by the outer ring on the inner one is 35.3 N and the maximal axial stiffness is $|K_z| = 6854$ N/m.
Moreover, the same kind of results is obtained when radially polarized ring magnets with alternate polarizations are stacked: the performances are the same as for axially polarized stacked rings.
So, as the radial polarization is far more difficult to realize than the axial one, these calculations show that it isn't interesting from a practical point of view to use radially polarized ring magnets to build bearings.
Nevertheless, this conclusion will be moderated by the next section. Indeed, the use of "mixed" polarization directions in a device leads to very interesting results.

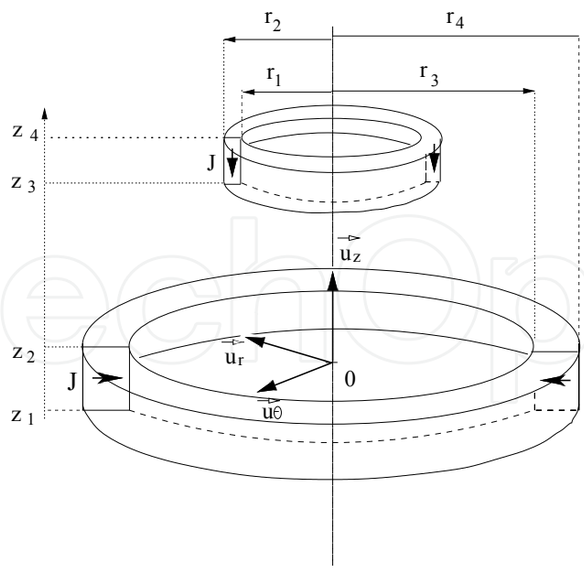

Fig. 24. Ring permanent magnets with perpendicular polarizations.

8. Determination of the force exerted between two ring permanent magnets with perpendicular polarizations

The geometry considered is shown in Fig. 24: two concentric ring magnets separated by a cylindrical air gap. The outer ring is radially polarized and the inner one is axially polarized, hence the reference to "perpendicular" polarization.

8.1 Notations

The following parameters are used:
r_1, r_2: inner and outer radius of the inner ring permanent magnet [m]
r_3, r_4: inner and outer radius of the outer ring permanent magnet [m]
z_1, z_2: lower and upper axial abscissa of the inner ring permanent magnet [m]
z_3, z_4: inner and outer axial abscissa of the outer ring permanent magnet [m]
The two ring permanent magnets are radially centered and their polarization are supposed uniformly radial.

8.2 Magnet modelling

The coulombian model is chosen for the magnets. So, each ring permanent magnet is represented by faces charged with fictitious magnetic pole surface densities. The outer ring permanent magnet which is radially polarized is modelled as in the previous section. The outer face is charged with the fictitious magnetic pole surface density $-\sigma^*$ and the inner one is charged with the fictitious magnetic pole surface density $+\sigma^*$. Both faces are cylindrical. Moreover, the contribution of the magnetic pole volume density will be neglected for simplifying the calculations.
The faces of the inner ring permanent magnet which is axially polarized are plane ones: the upper face is charged with the fictitious magnetic pole surface density $-\sigma^*$ and the lower one

is charged with the fictitious magnetic pole surface density $+\sigma^*$. All the illustrative calculations are done with $\sigma^* = \vec{J}.\vec{n} = 1$ T, where $\vec{J}$ is the magnetic polarization vector and $\vec{n}$ is the unit normal vector.

8.3 Force calculation

The axial force exerted between the two magnets with perpendicular polarizations can be determined by:

$$\begin{aligned} F_z &= \frac{J^2}{4\pi\mu_0}\int_{r_1}^{r_2}\int_0^{2\pi} H_z(r,z_3)rdrd\theta \\ &\quad -\frac{J^2}{4\pi\mu_0}\int_{r_1}^{r_2}\int_0^{2\pi} H_z(r,z_4)rdrd\theta \end{aligned} \tag{46}$$

where $H_z(r,z)$ is the axial magnetic field produced by the outer ring permanent magnet. This axial field can be expressed as follows:

$$\begin{aligned} H_z(r,z) &= \frac{J}{4\pi\mu_0}\int\int_S \frac{(z-\tilde{z})}{R(r_3,\tilde{\theta},\tilde{z})}r_3 d\tilde{\theta}d\tilde{z} \\ &\quad -\frac{J}{4\pi\mu_0}\int\int_S \frac{(z-\tilde{z})}{R(r_4,\tilde{\theta},\tilde{z})}r_4 d\tilde{\theta}d\tilde{z} \end{aligned} \tag{45}$$

with

$$R(r_i,\tilde{\theta},\tilde{z}) = \left(r^2 + r_i^2 - 2rr_i\cos(\tilde{\theta}) + (z-\tilde{z})^2\right)^{\frac{3}{2}} \tag{45}$$

The expression of the force can be reduced to:

$$\begin{aligned} F_z &= \frac{J^2}{4\pi\mu_0}\sum_{i,k=1}^{2}\sum_{j,l=3}^{4}(-1)^{i+j+k+l}\left(A_{i,j,k,l}\right) \\ &\quad +\frac{J^2}{4\pi\mu_0}\sum_{i,k=1}^{2}\sum_{j,l=3}^{4}(-1)^{i+j+k+l}\left(S_{i,j,k,l}\right) \end{aligned} \tag{44}$$

with

$$\begin{aligned} A_{i,j,k,l} &= -8\pi r_i\epsilon\mathbf{E}\left[-\frac{4r_ir_j}{\epsilon}\right] \\ S_{i,j,k,l} &= -2\pi r_j^2\int_0^{2\pi}\cos(\theta)\ln\left[\beta+\alpha\right]d\theta \end{aligned} \tag{43}$$

where $\mathbf{E}\left[m\right]$ gives the complete elliptic integral which is expressed as follows:

$$\mathbf{E}\left[m\right] = \int_0^{\frac{\pi}{2}}\sqrt{1-m\sin(\theta)^2}d\theta \tag{43}$$

The parameters ϵ, α and β depend on the ring permanent magnet dimensions and are defined by:

$$\begin{aligned} \epsilon &= (r_i - r_j)^2 + (z_k - z_l)^2 \\ \alpha &= \sqrt{r_i^2 + r_j^2 - 2r_i r_j \cos(\theta) + (z_k - z_l)^2} \\ \beta &= r_i - r_j \cos(\theta) \end{aligned} \tag{41}$$

8.4 Stiffness exerted between two ring permanent magnets with perpendicular polarizations

The axial stiffness derives from the axial force:

$$K_z = -\frac{d}{dz} F_z \tag{41}$$

where F_z is determined with $R(r_i, \tilde{\theta}, \tilde{z})$ and Eq. (46). After mathematical manipulations, the previous expression can be reduced in the following form:

$$K_z = \frac{J^2}{4\pi\mu_0} \sum_{i,k=1}^{2} \sum_{j,l=3}^{4} (-1)^{i+j+k+l} \left(k_{i,j,k,l} \right) \tag{41}$$

with

$$k_{i,j,k,l} = -\int_0^{2\pi} \frac{r_j (z_k - z_l)(\alpha + r_i)}{\alpha\,(\alpha + \beta)} d\theta \tag{41}$$

9. Study and characteristics of bearings using ring magnets with perpendicular polarizations.

9.1 Structures with two ring magnets

The axial force and stiffness are calculated for the bearing constituted by an outer radially polarized ring magnet and an inner axially polarized one. The device dimensions are the same as in section 7. Thus, the results obtained for this bearing and shown in Fig. 25 are easily compared to the previous ones: the maximal axial force is 39.7 N and the maximal axial stiffness is $|K_z| = 4925$ N/m.
So, the previous calculations show that the greatest axial force is obtained in the bearing using ring permanent magnets with perpendicular polarizations whereas the greatest axial stiffness is obtained in the one using ring permanent magnets with radial polarizations.

9.2 Multiple ring structures: stacks forming Halbach patterns

The conclusion of the preceding section naturally leads to mixed structures which would have both advantages of a great force and a great stiffness. This is achieved with bearings constituted of stacked ring magnets forming a Halbach pattern (Halbach, 1980).

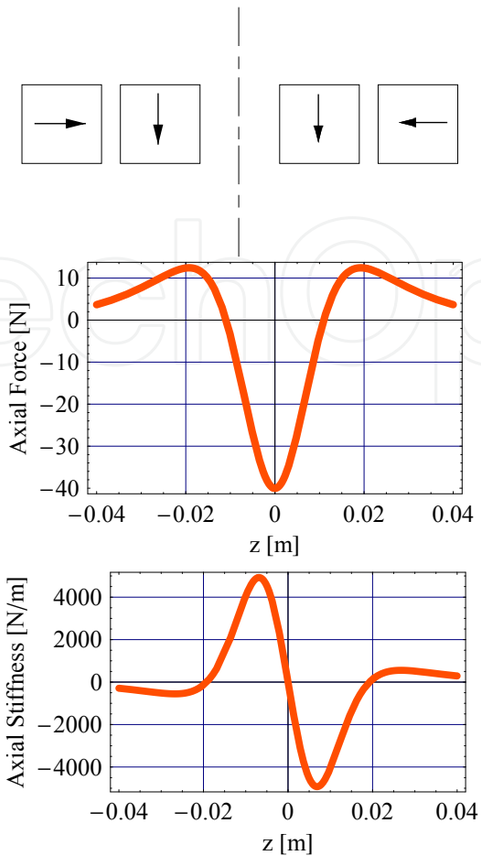

Fig. 25. Axial force axial stiffness versus axial displacement for two ring permanent magnets with perpendicular polarizations; $r_1 = 0.01$ m, $r_2 = 0.02$ m, $r_3 = 0.03$ m, $r_4 = 0.04$ m, $z_2 - z_1 = z_4 - z_3 = 0.1$ m, $J = 1$ T

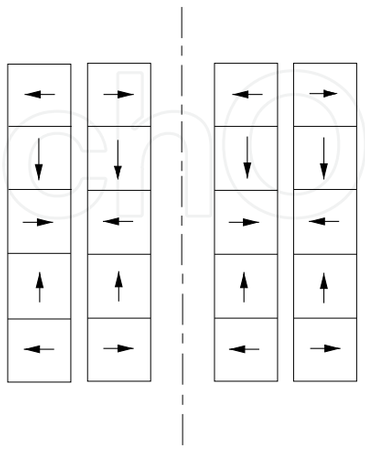

Fig. 26. Cross-section of a stack of five ring permanent magnets with perpendicular polarizations; $r_1 = 0.01$ m, $r_2 = 0.02$ m, $r_3 = 0.03$ m, $r_4 = 0.04$ m, $J = 1$ T, height of each ring permanent magnet = 0.01 m

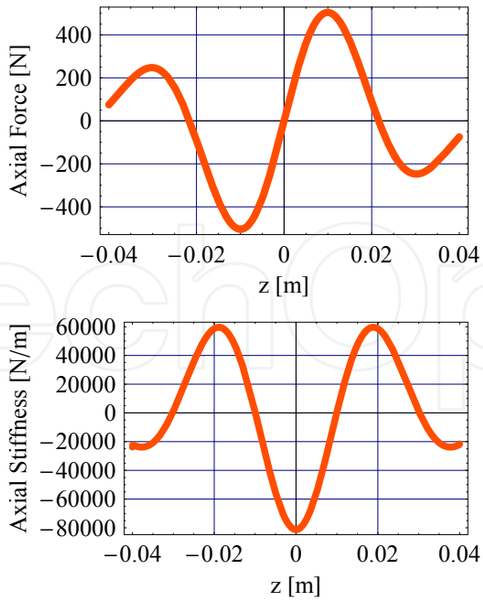

Fig. 27. Axial force and stiffness versus axial displacement for a stack of five ring permanent magnets with perpendicular polarizations; $r_1 = 0.01$ m, $r_2 = 0.02$ m, $r_3 = 0.03$ m, $r_4 = 0.04$ m, $J = 1$ T, height of each ring permanent magnet = 0.01 m

Section 4.2 shew that stacking ring magnets with alternate polarization led to structures with higher performances than the ones with two magnets for a given magnet volume. So, the performances will be compared for stacked structures, either with alternate radial polarizations or with perpendicular ones.
Thus, the bearing considered is constituted of five ring magnets with polarizations alternately radial and axial (Fig. 26). The axial force and stiffness are calculated with the previously presented formulations (Fig.27).
The same calculations are carried out for a stack of five rings with radial alternate polarizations having the same dimensions (Fig. 28). It is to be noted that the result would be the same for a stack of five rings with axial alternate polarizations of same dimensions.
As a result, the maximal axial force exerted in the case of alternate magnetizations is 122 N whereas it reaches 503 N with a Halbach configuration. Moreover, the maximal axial stiffness is $|K_z| = 34505$ N/m for alternate polarizations and $|K_z| = 81242$ N/m for the perpendicular ones. Thus, the force is increased fourfold and the stiffness twofold in the Halbah structure when compared to the alternate one. Consequently, bearings constituted of stacked rings with perpendicular polarizations are far more efficient than those with alternate polarizations. This shows that for a given magnet volume these Halbach pattern structures are the ones that give the greatest axial force and stiffness. So, this can be a good reason to use radially polarized ring magnets in passive magnetic bearings.

10. Conclusion

This chapter presents structures of passive permanent magnet bearings. From the simplest bearing with two axially polarized ring magnets to the more complicated one with stacked rings having perpendicular polarizations, the structures are described and studied. Indeed,

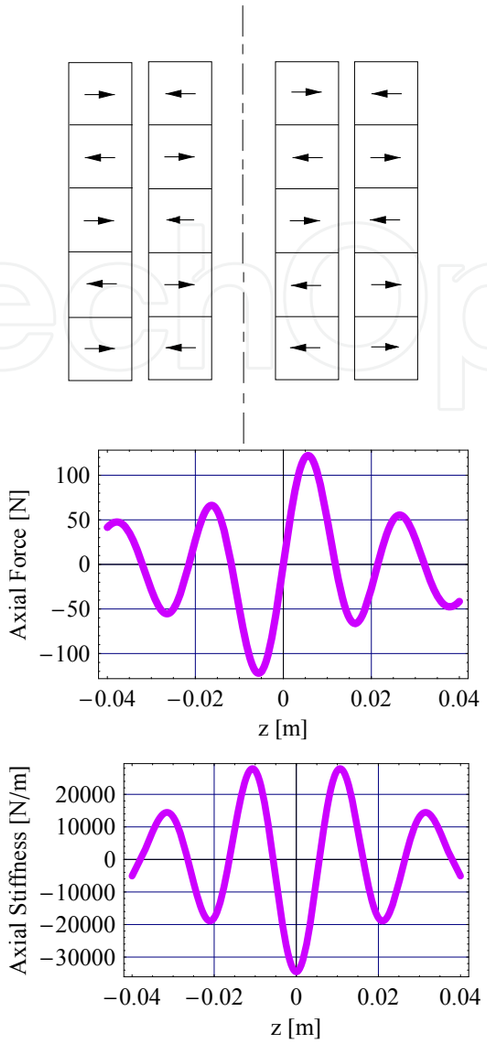

Fig. 28. Axial force and stiffness versus axial displacement for a stack of five ring permanent magnets with radial polarizations; $r_1 = 0.01$ m, $r_2 = 0.02$ m, $r_3 = 0.03$ m, $r_4 = 0.04$ m, $J = 1$ T, height of each ring permanent magnet = 0.01 m

analytical formulations for the axial force and stiffness are given for each case of axial, radial or perpendicular polarization. Moreover, it is to be noted that Mathematica Files containing the expressions presented in this paper are freely available online (*http://www.univ-lemans.fr/∼glemar*, n.d.). These expressions allow the quantitative study and the comparison of the devices, as well as their optimization and have a very low computational cost. So, the calculations show that a stacked structure of "small" magnets is more efficient than a structure with two "large" magnets, for a given magnet volume. Moreover, the use of radially polarized magnets, which are difficult to realize, doesn't lead to real advantages unless it is done in association with axially polarized magnets to build Halbach pattern. In this last case, the bearing obtained has the best performances of all the structures for a given magnet volume.

Eventually, the final choice will depend on the intended performances, dimensions and cost and the expressions of the force and stiffness are useful tools to help the choice.

11. References

Azukizawa, T., Yamamoto, S. & Matsuo, N. (2008). Feasibility study of a passive magnetic bearing using the ring shaped permanent magnets, *IEEE Trans. Magn.* **44**(11): 4277–4280.

Azzerboni, B. & Cardelli, E. (1993). Magnetic field evaluation for disk conductors, *IEEE Trans. Magn.* **29**(6): 2419–2421.

Babic, S. I. & Akyel, C. (2008a). Improvement in the analytical calculation of the magnetic field produced by permanent magnet rings, *Prog. Electromagn. Res. C* **5**: 71–82.

Babic, S. I. & Akyel, C. (2008b). Magnetic force calculation between thin coaxial circular coils in air, *IEEE Trans. Magn.* **44**(4): 445–452.

Barthod, C. & Lemarquand, G. (1995). Degrees of freedom control of a magnetically levitated rotor, *IEEE Trans. Magn.* **31**(6): 4202–4204.

Durand, E. (1968). *Magnetostatique*, Masson Editeur, Paris, France.

Filatov, A. & Maslen, E. (2001). Passive magnetic bearing for flywheel energy storage systems, *IEEE Trans. Magn.* **37**(6): 3913–3924.

Halbach, K. (1980). Design of permanent multiple magnets with oriented rec material, *Nucl. Inst. Meth.* **169**: 1–10.

Hijikata, K., Takemoto, M., Ogasawara, S., Chiba, A. & Fukao, T. (2009). Behavior of a novel thrust magnetic bearing with a cylindrical rotor on high speed rotation, *IEEE Trans. Magn.* **45**(10): 4617–4620.

Holmes, F. T. & Beams, J. W. (1937). Frictionnal torque of an axial magnetic suspension, *Nature* **140**: 30–31.

http://www.univ-lemans.fr/∼glemar (n.d.).

Hussien, A. A., Yamada, S., Iwahara, M., Okada, T. & Ohji, T. (2005). Application of the repulsive-type magnetic bearing for manufacturing micromass measurement balance equipment, *IEEE Trans. Magn.* **41**(10): 3802–3804.

Janssen, J., Paulides, J., Compter, J. & Lomonova, E. (2010). Threee-dimensional analytical calculation of the torque between permanent magnets in magnetic bearings, *IEEE Trans. Mag.* **46**(6): 1748–1751.

Kim, K., Levi, E., Zabar, Z. & Birenbaum, L. (1997). Mutual inductance of noncoaxial circular coils with constant current density, *IEEE Trans. Magn.* **33**(5): 4303–4309.

Lang, M. (2002). Fast calculation method for the forces and stiffnesses of permanent-magnet bearings, *8th International Symposium on Magnetic Bearing* pp. 533–537.

Lemarquand, G. & Yonnet, J. (1998). A partially passive magnetic suspension for a discoidal wheel., *J. Appl. Phys.* **64**(10): 5997–5999.

Meeks, C. (1974). Magnetic bearings, optimum design and applications, *First workshop on RE-Co permanent magnets, Dayton*.

Mukhopadhyay, S. C., Donaldson, J., Sengupta, G., Yamada, S., Chakraborty, C. & Kacprzak, D. (2003). Fabrication of a repulsive-type magnetic bearing using a novel arrangement of permanent magnets for vertical-rotor suspension, *IEEE Trans. Magn.* **39**(5): 3220–3222.

Ravaud, R., Lemarquand, G. & Lemarquand, V. (2009a). Force and stiffness of passive magnetic bearings using permanent magnets. part 1: axial magnetization, *IEEE Trans. Magn.* **45**(7): 2996–3002.

Ravaud, R., Lemarquand, G. & Lemarquand, V. (2009b). Force and stiffness of passive magnetic bearings using permanent magnets. part 2: radial magnetization, *IEEE Trans. Magn.* **45**(9): 3334–3342.

Ravaud, R., Lemarquand, G., Lemarquand, V. & Depollier, C. (2008). Analytical calculation of the magnetic field created by permanent-magnet rings, *IEEE Trans. Magn.* **44**(8): 1982–1989.

Ravaud, R., Lemarquand, G., Lemarquand, V. & Depollier, C. (2009). Discussion about the analytical calculation of the magnetic field created by permanent magnets., *Prog. Electromagn. Res. B* **11**: 281–297.

Samanta, P. & Hirani, H. (2008). Magnetic bearing configurations: Theoretical and experimental studies, *IEEE Trans. Magn.* **44**(2): 292–300.

Yonnet, J. P. (1978). Passive magnetic bearings with permanent magnets, *IEEE Trans. Magn.* **14**(5): 803–805.

Yonnet, J. P., Lemarquand, G., Hemmerlin, S. & Rulliere, E. (1991). Stacked structures of passive magnetic bearings, *J. Appl. Phys.* **70**(10): 6633–6635.

Magnetic Bearings, Theory and Applications

Edited by Bostjan Polajzer

ISBN 978-953-307-148-0

Hard cover, 132 pages

Publisher Sciyo

Published online 06, October, 2010

Published in print edition October, 2010

The term magnetic bearings refers to devices that provide stable suspension of a rotor. Because of the contact-less motion of the rotor, magnetic bearings offer many advantages for various applications. Commercial applications include compressors, centrifuges, high-speed turbines, energy-storage flywheels, high-precision machine tools, etc. Magnetic bearings are a typical mechatronic product. Thus, a great deal of knowledge is necessary for its design, construction and operation. This book is a collection of writings on magnetic bearings, presented in fragments and divided into six chapters. Hopefully, this book will provide not only an introduction but also a number of key aspects of magnetic bearings theory and applications. Last but not least, the presented content is free, which is of great importance, especially for young researcher and engineers in the field.

InTech Europe

University Campus STeP Ri
Slavka Krautzeka 83/A
51000 Rijeka, Croatia
Phone: +385 (51) 770 447
Fax: +385 (51) 686 166
www.intechopen.com

InTech China

Unit 405, Office Block, Hotel Equatorial Shanghai
No.65, Yan An Road (West), Shanghai, 200040, China
中国上海市延安西路65号上海国际贵都大饭店办公楼405单元
Phone: +86-21-62489820
Fax: +86-21-62489821

IntechOpen